Pure & Appl. Chem., Vol. 60, No. 5, pp. 675–684, 1988.
Printed in Great Britain.

Diagnostics of thermal plasma

V. Helbig

Institut für Experimentalphysik, Universität Kiel, D 2300 Kiel, Germany

Abstract - The state of complete thermodynamic equilibrium (TE) can only be established in a plasma, when it is enclosed in a cavity with walls kept at a fixed temperature. Once the cavity is removed, the plasma will lose energy by heat currents, diffusion processes and radiation. In order to compensate for these losses, the plasma has to be heated continuously. This will cause gradients of all plasma parameters. It is obvious, that such a system is no longer in complete TE. It is therefore the first step in plasma diagnostics, to get information about the actual state of the respective plasma. In the following a number of different experimental techniques as e.g. emission spectroscopy, interferometry and laser light scattering are discussed. The desired plasma parameters can be obtained from the results of the various measurements, when the appropriate plasma model is known.

INTRODUCTION

For the analysis of a given plasma a number of experimental techniques are available. Intensities of isolated lines and the continuum from emission spectroscopy primarily give information about number densities of atomic and ionic excited states and the electrons. Studies of the broadening and shift of spectral lines yield the electron density as well. Interferometric measurements with lasers monitor the index of refraction of the plasma which is correlated again with the number densities. Thomson scattering gives information about the electron density if one measures the total amount of the scattered light. From the shape of the observed spectrum the electron temperature can be obtained. This short survey, which of course is incomplete, characterizes the situation that the observed quantities in most cases give the densities while information about the temperature requires usually a model connecting number densities and temperature.

THE PLASMA STATE

Plasma models are an important aid in plasma diagnostics. With their help it is possible to describe the physical state of the plasma to a certain degree of approximation using a small number of state parameters. Especially in the case of a plasma in complete thermodynamic equilibrium the situation is quite simple. The state of the plasma is fully described by the pressure, the temperature and the chemical composition. There exists a Maxwellian distribution of the velocities f(v); the distribution of ions and atoms over their various excited states is given by the Boltzmann energy distribution exp(-E/kT); the ratio of the number densities of subsequent ionic states is obtained from Saha's equation S(T) and the spectrum is given by Planck's radiation law $B_\nu(T)$. It is specific for the TE state that every microscopic process is balanced by its inverse. This principle of detailed balancing may be used to derive the TE relationships. It is obvious that for laboratory plasmas this balance cannot be maintained. The losses by radiation and heat fluxes cannot be compensated by the inverse process but it will be necessary to balance them through different channels in order to sustain the plasma, usually by Ohmic heating. The consequence is that gradients of nearly all quantities will occur that drive diffusion processes. Even though in laboratory plasmas the TE state is seldom realized, this model is of considerable importance, as a number of TE relations still are effective when others already fail. A very powerful concept is that of local thermodynamic equilibrium (LTE). It describes a state that is in complete TE with exception of the radiation field which is deluted compared to the black-body value ($I_\nu \leq B_\nu(T)$). The LTE model is the basis of most of the diagnostic work done with laboratory plasmas. It is expected to hold, if collisional processes of the electrons dominate the rate equations and thus compensate for the radiation losses. Next in the hierarchy of plasma states is the model of partial local thermodynamic equilibrium (PLTE), which is defined by an under-population of the excited states and the drop of the kinetic temperature of the heavy particles below the value of the electron temperature. Thus for the PLTE state two additional parameters are necessary to describe the plasma state. The under-population factor $b \leq 1$ for excited levels m is defined by

$$N_m = b\, N_m^{LTE}$$

and the different kinetic temperatures may be described by

$$\beta = T_g / T_e$$

where T_g and T_e are the heavy particle and electron temperature, respectively. As the atoms in the excited states are in equilibrium with the free electrons the under-population factor enters also Saha's equation

$$S(T_e) = b\, S(T_e)^{LTE}.$$

Figure 1 shows the results of the analysis of the state of an argon arc at atmospheric pressure (ref. 1). The temperature derived from different methods takes different values for arc currents lower than I = 40 A corresponding to an electron density of $N_e = 7\ 10^{16}$ cm^{-3} (refer to Fig. 6). This indicates deviations from the LTE state.

The dashed line, denoted T_{LTG}, gives the temperature calculated from the known total pressure and the electron density obtained from interferometric measurements (ref. 2). To derive this temperature LTE has been assumed in so far, as no under-population of the excited levels was taken into account. To relate the number densities to the pressure, however, different temperatures were used for the electrons and the heavy particles.

The determination of the electron temperature is somehow problematic. It was assumed that the free electrons follow a Maxwellian velocity distribution and that the population of the highly excited argon states are in equilibrium with the free electrons. The combined Saha-Boltzmann equation relates the measured intensity of a spectral line and the electron density under these assumptions with a temperature that is called electron temperature in Fig. 1. It is interesting to observe, that the temperature derived according to this scheme is different for different spectral lines (λ = 430.0 nm (●), λ = 714.7 nm (⊙)) for arc currents lower than I = 15 A (see discussion below).

The temperature of the heavy particles T_g was obtained from two different methods. As was first observed by Gurevich et al. (ref. 3) the intensity of a spectral line emitted from a non-thermal gas discharge increases for the first several microseconds after interruption of the current (refer to Fig. 2). This may be explained by the fact that the time necessary for rethermalization of the electrons at the new (lower) temperature of the heavy particles is much smaller than the time required for recombination with the ions. Therefore one can assume that the electron density remains constant for the first moment after interruption of the current. In this case the the intensity of the line is given by

$$I \sim N_m \sim N_e^2\ T^{-3/2}\ \exp\{(E_\infty - E_m)/kT\}$$

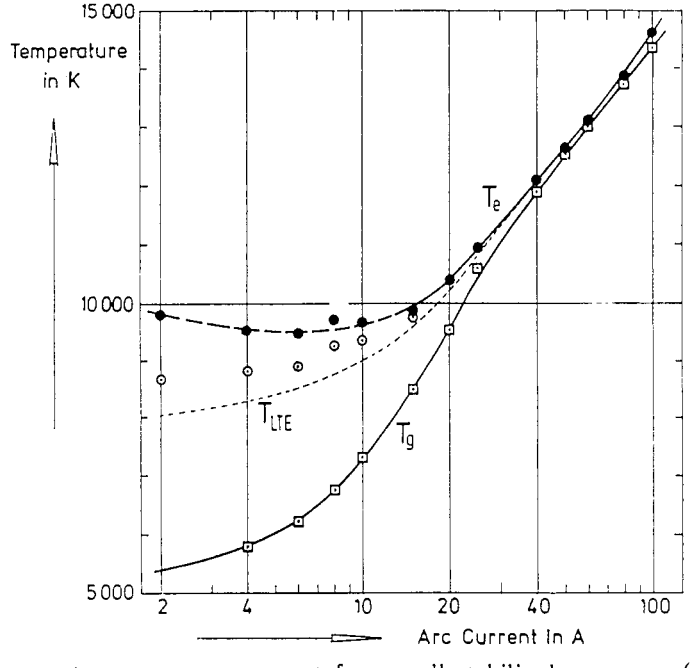

Fig. 1. Temperature versus arc current for a wall-stabilized argon arc (ref. 1). T_{LTG} is calculated from the electron density obtained from interferometric measurements. T_e is obtained from line intensities and N_e. The heavy particle temperature has been derived from line intensity jumps following interruption of the arc current and from the energy balance for the free electrons (ref. 2).

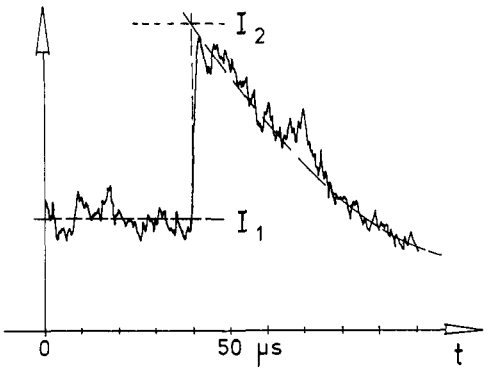

Fig. 2. Intensity jump of a spectral line observed after short-circuiting the arc (ref. 2).

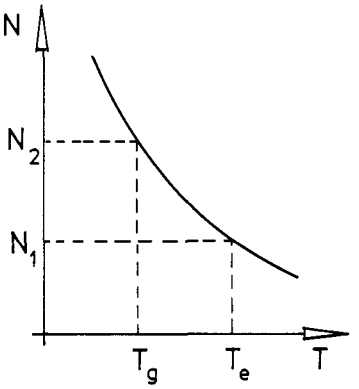

Fig. 3. Number density of an excited level versus temperature. Under the assumption that N_e is constant one obtains higher N_m values when the temperature becomes lower.

Figure 3 shows the number density N_m of the upper level of a line with the excitation energy E_m versus the temperature for constant N_e. An increase of N_m with decreasing temperature is observed. With the begin of the recombination the intensity will of course drop below the initial value as one can see from Fig. 2. From the height of the intensity jump in Fig. 2 the ratio of electron to heavy particle temperature can be obtained which yields directly T_g if T_e is known.

Another method for determining the heavy particle temperatures makes use of the energy balance of the free electrons. The energy deposited in the electron gas of the plasma by Ohmic heating is dissipated by elastic collisions with the heavy particles, by electron heat conductivity, by ambipolar diffusion and by radiation losses

$$\sigma E^2 = 3 (m_e / m_A) (T_e - T_g) k N_e \nu_{e-A}^{coll.} + W_{heat} + W_{diff.} + W_{rad.}.$$

Only the collision term is given explicitly as it is the one where the difference of the respective temperatures enters. The quantities necessary to solve this equation for the temperature difference e.g. the cross-sections, the electrical and thermal conductivity, the coefficient of ambipolar diffusion and the radiation losses were taken from the literature (for details we refer to Nick ref. 2). The radial distributions of the electron density and the electron temperature enter the terms for thermal conductivity and for ambipolar diffusion. These were obtained from side-on measurements on the arc plasma. The result for the electron density for a current of I = 15 A is shown in Fig. 4. The electron density profile measured directly from the absolute continuum intensity is compared with the one calculated from the electron temperature profile obtained from line intensity measurements. Diffusion causes electron losses at the arc axis that appear as surplus of electrons in the outer part of the discharge. This again confirms that the arc plasma at the specified electron density is not in the state of LTE. Figure 5 shows a similar radial profile for a higher current, where the LTE relations are applicable for the arc axis. Solving the energy balance with the measured density and temperature profiles and the electric fieldstrength yields the heavy particle temperature. The average of the results from both methods is given in Fig. 1.

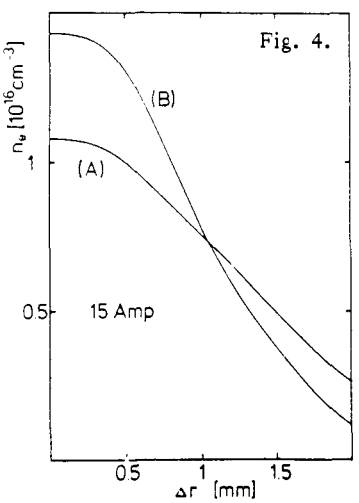

Fig. 4. Radial distribution of the electron density of an argon arc at I = 15 A. (A) determined from the absolute intensity of the argon continuum. (B) calculated from the electron density using LTE relations (from ref. 2).

Fig. 5. Radial distribution of the electron density of an argon arc at I = 40 A. (A) and (B) as in Fig. 4.

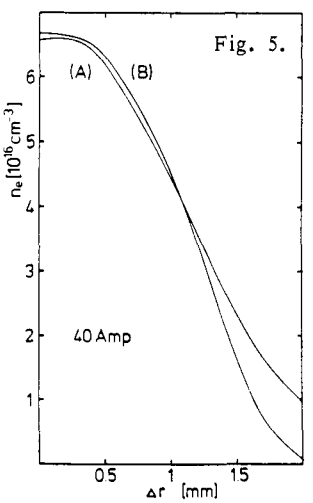

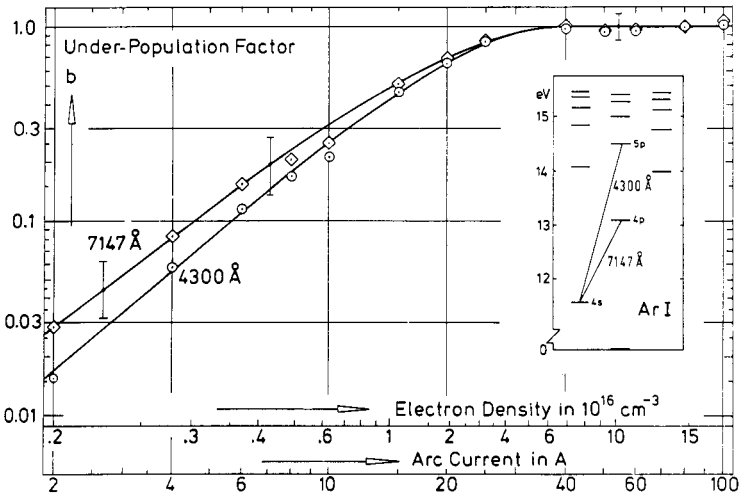

Fig. 6.
The under-population factor b for two argon lines plotted versus the electron density.

TABLE 1. Possible deduced states of a non-LTE nitrogen plasma if LTE is assumed. The underlined quantities were used to calculate the others given in table (see text).

Measured quantities	P (atm)	$N_e \times 10^{-16}$ (cm^{-3})	$N_0^* \times 10^{-10}$ (cm^{-3})	$N_1^* \times 10^{-9}$ (cm^{-3})	T (K)
P, NI	0.2	2.6	7.8	0.012	12000
P, NII	0.2	4.4	12	1.2	15000
NI, NII	0.16	3.8	7.8	1.2	15200
NI, N_e	0.26	5.0	7.8	51	19200
NII, N_e	0.23	5.0	15	1.2	14900

In Fig. 6 the under-population factor b, as derived from the analysis of the argon plasma, is plotted versus the electron density for two different argon lines. b = 1 indicates the LTE state. Between $N_e = 7\ 10^{16}$ cm^{-3} and approximately $N_e = 1\ 10^{16}$ cm^{-3} the under-population of the 4p and 5p levels can be described by one common b-factor. Below an arc current of I = 15 A the two levels show different under-population. It is clear from Fig. 2 that reducing the data under the assumption of LTE for electron densities too low for establishing equilibrium may lead to drastic errors in the number densities.

Table 1, compiled from data given by Shumaker (ref. 4), illustrates how the assumption of LTE can influence the determination of the plasma parameters in a non-LTE situation. In ref. 4 a nitrogen plasma was studied. The total pressure, the electron density from a Stark-broadened line and the intensities of an atom- and an ion-line were measured. Assuming LTE the temperature and the two remaining quantities were calculated from each pair of the experimental values. The values of the quantities used to calculate the remainder are underlined in the table. If, for example, only the total pressure and the neutral line intensity were measured, the deduced electron density and excited ionic-state population would be lower than the observed ones by factors of 2 and 100, respectively. The temperature, which was not measured directly, ranges between 12 000 and 19 200 K.

All the plasmas discussed in this chapter contained only one element. This is the most simple case one can think of. Even then it was shown that the number of parameters necessary to describe the plasma increases when LTE is not established. In more complex plasmas the situation becomes worse, especially as new mechanisms that drive diffusion fluxes have to be considered.

EMISSION SPECTROSCOPY

Line intensities

The local emission and absorption determines the radiation emitted from a plasma. When no re-absorption occurs, one obtains the emitted radiation simply by summation over the emission coefficients of all volume elements along the line of observation. Generally, however, one has to consider the absorption too. This leads to the equation of radiative transfer. Introducing the optical depth τ_λ and the source function S_λ this equation reads

$$dI_\lambda / d\tau_\lambda = S_\lambda - I_\lambda \ .$$

For a homogeneous plasma with the length s and the absorption coefficient $\varkappa_\lambda$ the optical depth becomes

$$\tau_\lambda = \varkappa_\lambda \cdot s$$

and the source function is given by

$$S_\lambda = \varepsilon_\lambda / \varkappa_\lambda$$

where ε_λ is the coefficient for spontaneous emission. In the case of LTE the source function is equal to Planck's radition law. In the following we will consider only the simple case of a homogeneous plasma. The solution of the equation of radiative transfer is then given by

$$I_\lambda = S_\lambda \{1 - \exp(-\tau_\lambda)\} .$$

Very large and very small values of the absorption coefficient lead to the limiting cases

$$\varkappa_\lambda \, s \ll 1 : \; I_\lambda = \varkappa_\lambda \, s \quad \text{(optically thin)}$$

$$\varkappa_\lambda \, s \gg 1 : \; I_\lambda = S_\lambda \quad \text{(optically thick).}$$

Homogeneous and optically thin layer. In this case the line intensity is given by

$$I_L = \int I_\lambda \, d\lambda = s \int \varepsilon_\lambda \, d\lambda = h \, c \, s \, A_{nm} \, N_m / (4\pi\lambda)$$

where A_{nm} is the Einstein coefficient, N_m the number density of the atoms in the upper level and λ the wavelength of the transition. For a LTE plasma the number density of the excited state is a known function of the temperature which can be determined in this case from the absolute line intensity when the Einstein coefficient is known.

Optically non-thin layer. Intensities close to or equal to the blackbody radiation given by Planck's radiation law may be reached in the centre of strong emission lines. Especially the resonance lines of the various elements tend to have an optically thick line core. If the resolution of the spectrometer is sufficient to resolve the true line profile, the absolute peak intensity can be used to calculate the electron temperature in a LTE plasma (refer to ref. 1). This method has the advantage that no atomic constants need to be known. The drawbacks are, that the resolution necessary is very high, that the method is very sensitive to absorption in colder layers and that the result for the temperature depends critically on the accuracy of the absolute spectral calibration.

Figure 7 shows two scans of a carbon I multiplet in the vacuum-UV region of the spectrum recorded with an arc source. If no precautions are taken, these strong resonance lines even appear, when the arc is operated in pure argon (Fig. 7 a). Few per cent admixture of CO_2 will bring the line cores to the blackbody limit as indicated in Fig. 7 b. This figure has been included to demonstrate the difficulties one can get if the two limiting cases discussed above are used to interpret emission spectra. In Fig. 7 a even the weakest of the six lines is close to one half of the blackbody intensity as estimated from Fig. 7 b. This will require corrections for optical thickness when the line intensities are determined. In Fig. 7 b the six lines are re-absorbed in cold layers outside the arc plasma. In this case it will be difficult to judge to what extend absorption in the line wings has lowered the blackbody intensity.

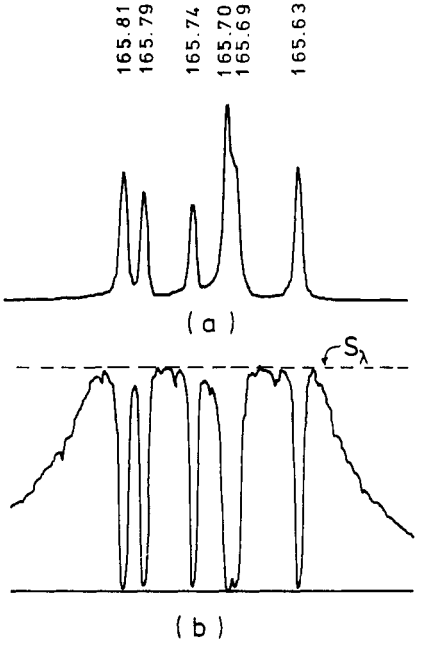

Fig. 7. Vacuum-UV spectrum of the CI - multiplet at 165 nm. (a) spectrum of the argon arc with no admixture. (b) argon with an admixture of 5% CO_2.

Line profiles

The profile of a spectral line is influenced by a number of broadening mechanisms. For thermal plasmas Stark broadening usually is the dominant effect. At low electron densities and for transitions close to the core, however, Doppler broadening may be considerable too. Broadening by neutrals is of minor importance unless the total pressure is very high. Determination of plasma parameters from the line profile is straightforward when the line is emitted

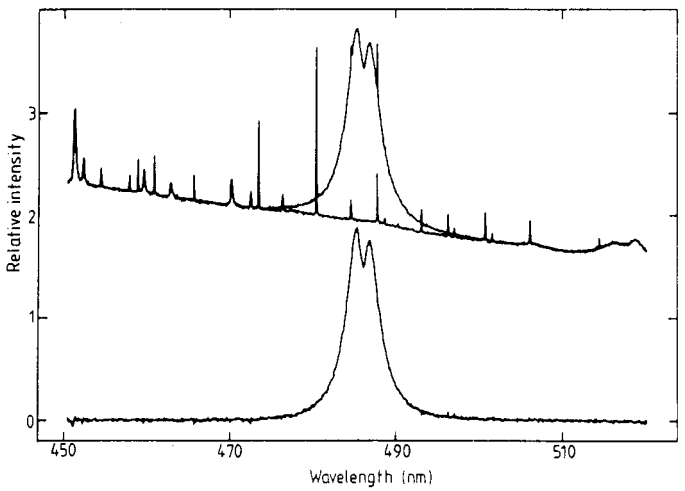

Fig. 8. H β spectrum from an argon arc with small admixtures of hydrogen. Upper trace shows the spectrum of the gas-mixture and the pure argon arc. The lower trace shows the difference, that represents the hydrogen contribution (from ref. 5).

from an optically thin and homogeneous layer and the resolution of the spectrometer is sufficient. In case that these conditions are not met the line profile will be distorted and deconvolution procedures will be necessary to recover the true shape of the line.

Stark broadening. The broadening of spectral lines by Stark effect offers a simple method to obtain the electron density in a plasma. Especially broad lines are caused by the linear Stark effect of the hydrogen lines. Here the first members of the Balmer series have received special attention. In case of linear Stark effect the half-width increases with $N_e^{2/3}$

$$\Delta\lambda_{1/2} = C(N_e, T_e)\, N_e^{2/3}$$

where C depends weakly on the electron density and the electron temperature. Figure 8 shows a spectrum of the Balmer Beta line (refer to ref. 5). The line profile is complex and cannot be described by an analytical function. It shows a central minimum that follows from the static Stark effect pattern and not from reabsorption. In ref. 5 the half-width of this line has been calibrated with electron densities obtained from interferometric measurements (see discussion below and Fig. 14). Excellent agreement with the calculations of Vidal et al. (ref. 6) has been obtained. Presumably the Stark broadening parameter of this line is the best known.

The spectral lines of all other elements (with exception of very few helium lines) exhibit quadratic Stark effect. In this case the half-width is proportional to the electron density

$$\Delta\lambda_{1/2} = C(N_e, T_e)\, N_e \ .$$

The broadening caused by the quadratic Stark effect usually is much smaller than that from the linear Stark effect. Figure 9 shows the Stark parameter for a prominent argon line plotted versus the electron density. At low values of N_e the observed profile is influenced by the finite width of the spectrometer and by the Doppler effect. At high electron densities the measurement of the width becomes difficult because the wings of neighboring lines prevent an exact determination of the background. This is illustrated by Fig. 10 where a scan of the argon spectrum in the vicinity of this line is shown for two different electron densities.

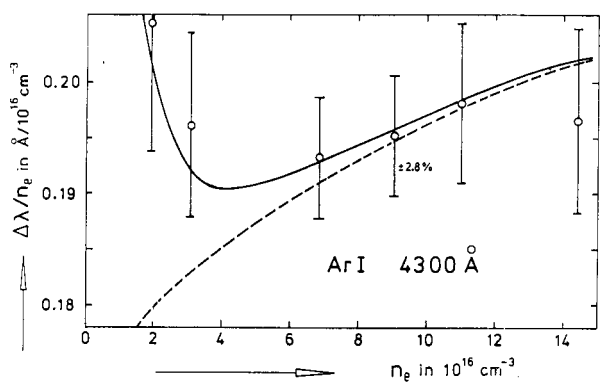

Fig. 9. The reduced half-width of the Stark-broadened Ar I line at λ = 430.0 nm plotted versus the electron density. The broken line gives the contribution of the Stark effect to the width. The full line gives the convolution of the Stark profile with Doppler- and apparatus profile. The measured widths follow this curve very closely.

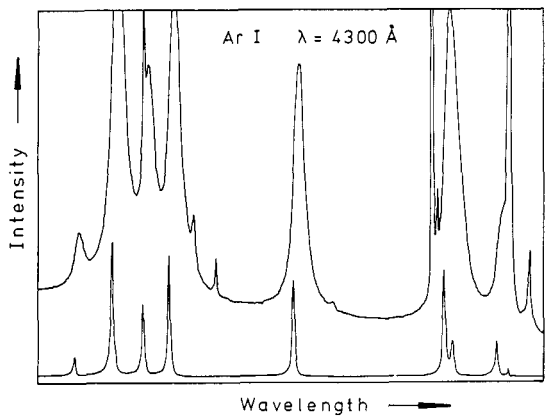

Fig. 10. Part of the argon spectrum in the vincinity of the Ar I line at λ = 430.0 nm for two different electron densities. The upper spectrum corresponds to $N_e = 1.46\ 10^{17}$ cm^{-3} and the lower one to $N_e = 3.15\ 10^{16}$ cm^{-3}.

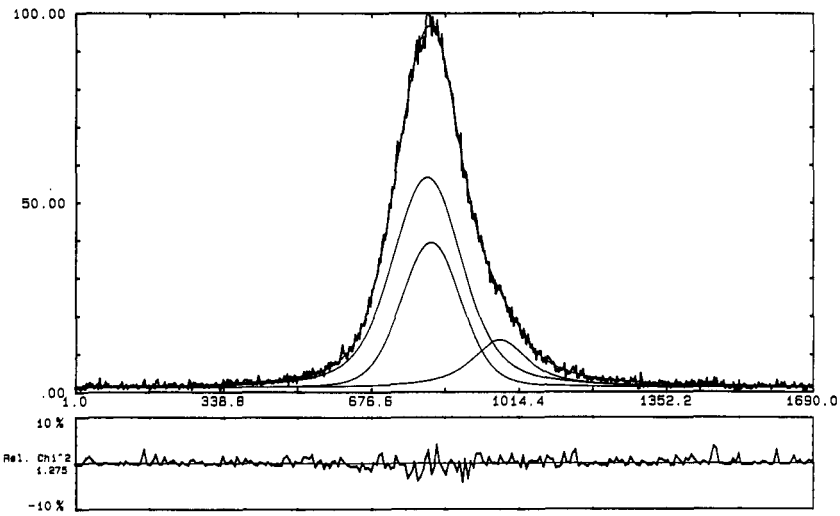

Fig. 11. Spectrum of the He I line at λ = 471.3 nm emitted from a helium arc at an electron density of $N_e = 1.2\ 10^{15}$ cm^{-3}. The experimental profile was fitted to the sum of the three triplet components. The quality of the fit can be judged from the residue below the spectrum.

Doppler broadening. The profile of a purely Doppler-broadened line has a Gaussian shape with the half-width given by

$$\Delta\lambda_{1/2} = 2\ \lambda/c \sqrt{2\ \ln 2\ k\ T_g\ /\ m}\quad .$$

Doppler broadening is expected to be most pronounced for light elements at high temperatures. Figure 11 shows as an example the spectrum of the helium line λ = 471.3 nm emitted from an arc plasma at an electron density of $N_e = 1.2\ 10^{15}$ cm^{-3}. The line from the triplet system of helium was chosen as one being fairly insensitive to the Stark effect. A computer routine was used to fit the sum of three profiles to the experimental data. Center wavelength, intensity, Gaussian width and Lorentzian width were free fitting parameters for each line. The heavy particle temperature was obtained from that profile with an uncertainty of less than ± 5 %.

INTERFEROMETRY

The index of refraction n of a plasma is given by

$$(n-1)_{Pl} = (n-1)_A + (n-1)_I + (n-1)_e$$

where A, I and e denote the contribution to the refractivity of the atoms, ions and electrons, respectively. The contribution of the excited species are neglected in the balance. It was shown in ref. 7 that the error introduced by this approximation never exceeds 2.5 % for hydrogen or argon under conditions typical for arc plasmas. The refractivity for the heavy particles is given by a dispersion-type formula

$$(n-1)_{A,I} = 2\pi e^2/m \sum_{m,n} N_m f_{mn} /(\omega_{mn}^2 - \omega^2).$$

The index of refraction of the electrons is described by

$$(n-1)_e = 2\pi e^2 N_e /m\omega^2.$$

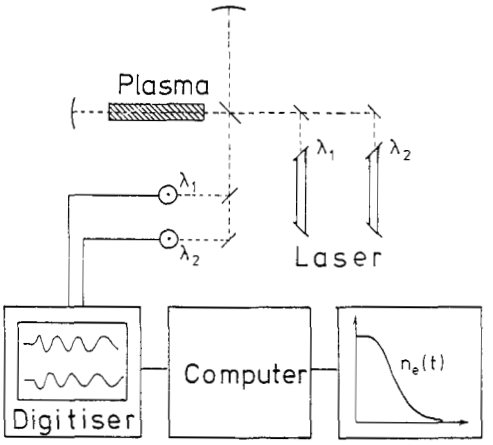

Fig. 12· Experimental set-up for measuring the plasma electron density with a two-wavelength laser interferometer (schematic).

The influence of the atoms and the ions can be eliminated, if the index of refraction e.g. of a homogeneous arc plasma is measured with two lasers of different wavelengths and one assumes, that only singly charged ions are present in the plasma.

A typical experimental set-up is shown in Fig. 12. The plasma is in one arm of a Michelson interferometer. Two laser with different wavelengths are used to measure the change of the plasma refractivity after short-circuiting the arc by means of a thyristor. The fringes at the exit of the interferometer are recorded with a transient digitiser and the phase shifts are determined as function of the time elapsed since interruption of the plasma. From these data the change of the electron density can be calculated. When all electrons have recombined no change of N_e is observed any longer. The difference to the value before switching off the arc gives the electron density.

A set of real interference fringes for a krypton plasma from ref. 8 is shown in Fig. 13 where the different steps from the aquisition of an interferogram to the computation of the electron density are indicated. The raw data from the transient digitiser consist of two envelopes for each set of fringes for the two wavelengths λ = 1152.3 nm (upper trace) and λ = 632.8 nm (lower trace).

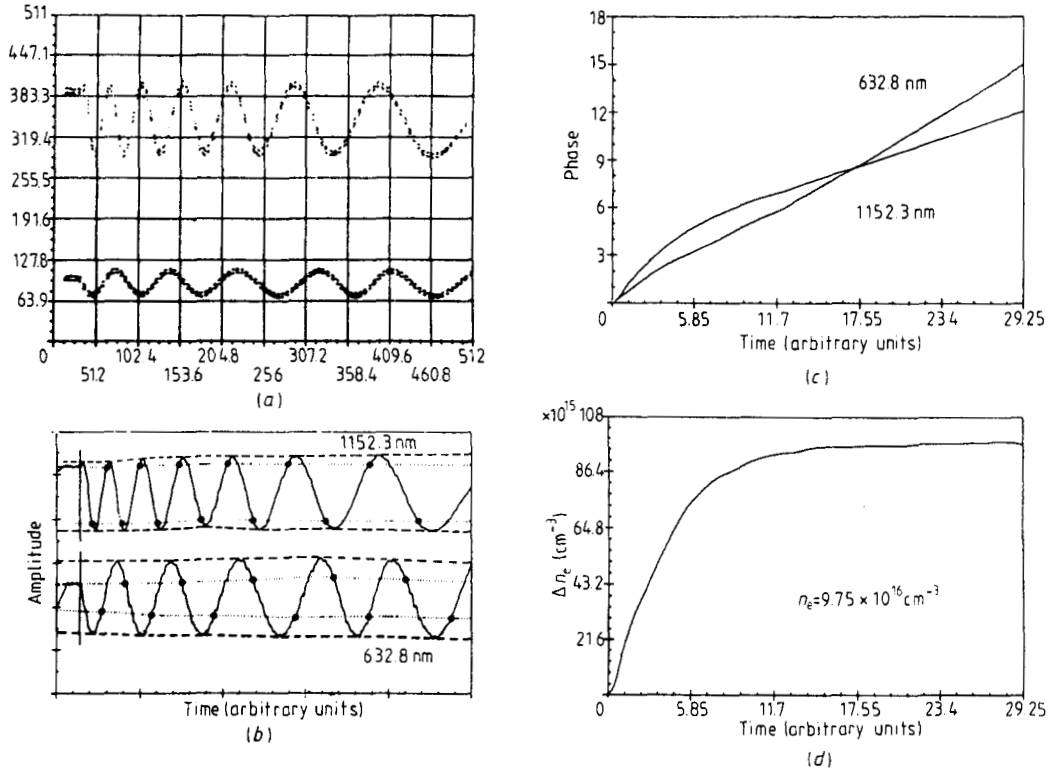

Fig. 13. Scheme of the interferometric electron density determination. (a) Raw data from the transient digitiser. (b) Evaluation of the phase values. (c) Change of the phase plotted against time. (d) Change of the electron density after cut-off of the arc current.

By software procedures these two curves were separated. normalised and corrected for geometric distortions. As indicated in Fig. 13 b. the phase values were read off at full and half cycles. These manually received values were used to calculate the temporal change of the phase with the help of a spline interpolation routine as shown in Fig. 13 c. Still another computer program determined the electron density change from these curves. Several factors contribute to the uncertainty of the electron density obtained by this procedure. As one can see the plateau reached in Fig. 13 d is not a perfect straight line. Besides that. the length of the plasma is not known to better than 2 %. A careful error analysis lead to an accuracy of better than 5 %. In more favourable cases uncertainties of less than 2 % are reported (ref. 5).

In deriving number densities from interferometric measurements no assumptions about the state of the plasma are necessary. As this method yields the electron density with high precision, it was used to calibrate the halfwidth of Hβ over a wide range of electron densities (ref. 5 and 9). The results are shown in Fig. 14 where the reduced halfwidth of the Balmer Beta line is plotted versus electron density. The measurements at low densities (●) were obtained in a helium arc with small admixtures of hydrogen using as laser wavelengths the He-Ne laser line at 0.6 μ and the CO_2 laser wavelength at 10.6 μ . The values for the higher electron densities (○) were measured in an argon arc with trace amounts of hydrogen using the He-Ne laser wavelengths at 0.6 and 1.15 μ . Theoretical results of Vidal et al. (ref. 6) using the unified theory are also shown for comparison. There is an excellent agreement between the experimental and the theoretical results in the whole electron density range spanning more than two decades. These results are in contradiction to the investigation of Goode and Deavor (ref. 10) who found for the Balmer Beta line 'that the half-width method exhibits substantial systematic errors, generally over-estimating electron density by a factor of 2-3' compared to a least-squares analysis of the whole profile.

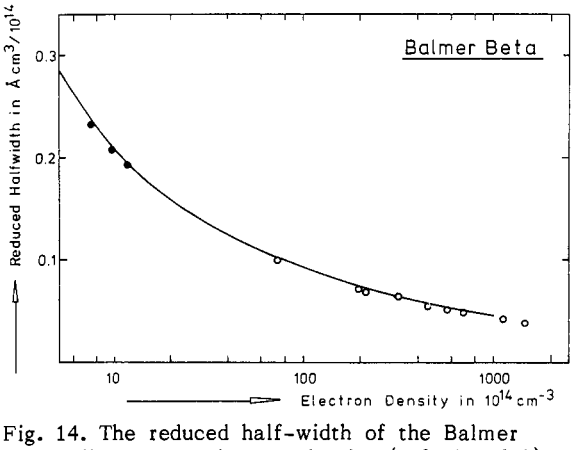

Fig. 14. The reduced half-width of the Balmer Beta line versus electron density (ref. 5 and 9). For comparison the theoretical values of Vidal et al. (ref. 6) are included.

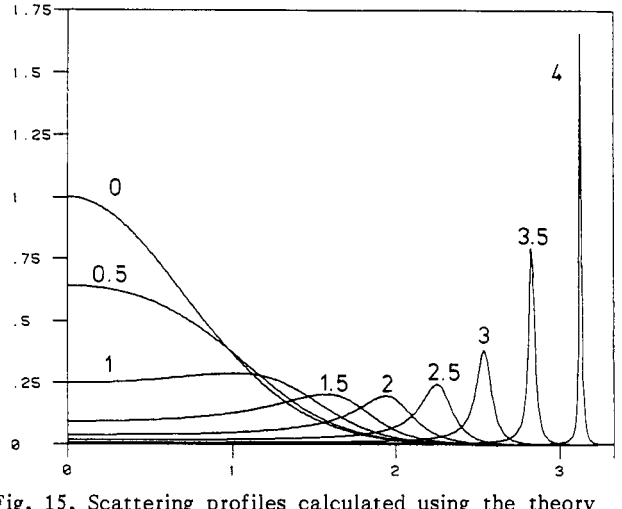

Fig. 15. Scattering profiles calculated using the theory of Salpeter for the α - parameters indicated (ref. 12).

SCATTERING OF LASER LIGHT

The spectrum of the light scattered by a plasma is determined by the spectral distribution of the density fluctuations. It can be characterized by the parameter

$$\alpha = \lambda \cdot (4\pi\lambda_D \sin\theta/2)^{-1}$$

where λ is the wavelength of the incident light, λ_D the Debye length and θ the scattering angle. Using the theory of Salpeter (ref. 11) one can calculate a set of profiles for different values of the scattering parameter. Results of such calculations are shown in Fig. 15 (ref. 12).

One can discuss two limiting cases. For $\alpha \ll 1$ one obtains a profile that has nearly a Gaussian shape

$$I(\Delta\lambda) = I(0) \exp\{-(\Delta\lambda/\Delta\lambda_{1/2})^2\}$$

where the halfwidth is given by

$$\Delta\lambda_{1/2} = 4 \sin\theta/2 \cdot \lambda/c \cdot \sqrt{2 \ln 2 \; k T / m}$$

If high precision is required one has to take into account the deviations of the scattering profile from a Gaussian even for small values of α. Brandt (ref. 12) has given a procedure to correct for these small differences for scattering parameters up to approximately $\alpha \cong 0.7$.

For α - values greater than one satellites appear in the spectrum (refer to Fig. 15). Information about the electron density is contained in the position of the satellites. If these are well separated from the central line the reduction of the data is simple. For high density plasmas with moderate temperatures (e.g. arc discharges) the scattering parameter unfortunately is of the order of one. This requires a detailed comparison of the experimental line profile with the calculated ones.

The absolute integrated line intensity of the scattering profile leads to the electron density. In order to eliminate all influences of the experimental set-up the Thomson spectra usually are calibrated with Rayleigh signals from scattering in the cold gas where the cross-sections are accurately known

$$\frac{N_e}{N_0} = \frac{\sigma_R \int I_{Th}\, d\lambda}{\sigma_{Th} \int I_R\, d\lambda}$$

N_e and N_0 are the electron and cold gas densities (e.g. argon or nitrogen), the σ are the respective cross-sections and the integrals give the line intensities.

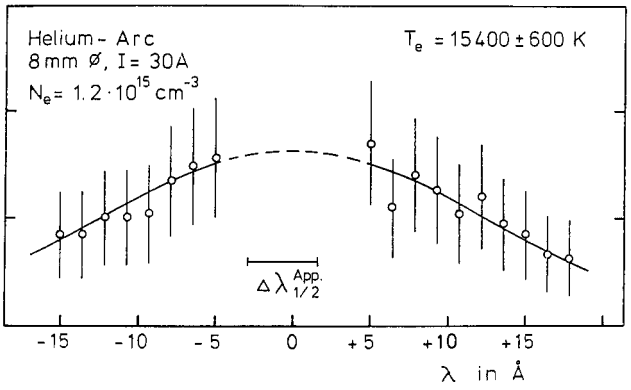

Fig. 16. Intensity versus wavelength of a scattering spectrum from a helium arc plasma. The α - parameter was 0.24 (ref. 12).

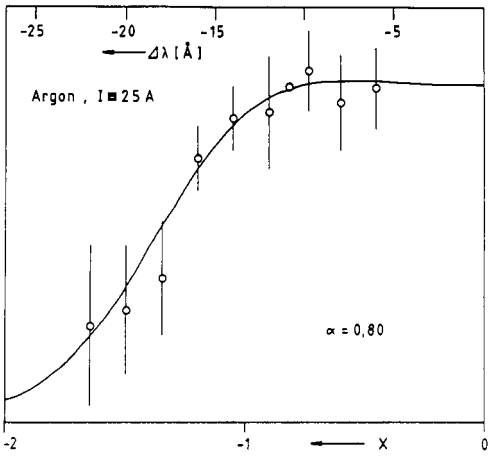

Fig. 17. Intensity versus wavelength of a scattering spectrum from an argon arc plasma. The α - parameter was 0.80 (ref. 12).

Results from a scattering experiment using a CW-Laser are shown in Fig. 16 and 17 (ref. 12). The arc plasma was placed inside the cavity of an argon-ion laser operating at the green line at 514.5 nm. As it was essential to obtain good spatial resolution focussing mirrors were incorporated in the resonator. To discriminate against the strong continuous background of the arc plasma lock-in detection was employed. The results for a helium plasma with $\alpha = 0.24$ are given in Fig. 16. Figure 17 shows a profile from an argon plasma where the α parameter is 0.80. The electron density obtained from the intensity of this profile is in close agreement with interferometric results for the same plasma conditions determined by Nick (ref. 2) showing the consistency of the different diagnostic methods.

REFERENCES

1. K.-P. Nick, J. Richter, and V. Helbig, J. Quant. Spectrosc. Radiat. Transfer 32, 1 (1984).
2. K.-P. Nick, Thesis, Kiel (1982).
3. D.B. Gurevich and I.V. Podmoshenskii, Opt. Spectrosc. 18, 319 (1963).
4. J.B. Shumaker, J. Quant. Spectrosc. Radiat. Transfer 14, 19 (1974).
5. V. Helbig and K.-P. Nick, J. Phys. B 14, 3573 (1981).
6. C.R. Vidal, J. Cooper, and E.W. Smith, Astrophys. J. Suppl. 25, 37 (1973).
7. V. Helbig and K.-P. Nick, Proc. of the XVII Int. Conf. on the Phenomena in Ionized Gases, Budapest (1985).
8. T. Brandt, V. Helbig and K.-P. Nick, J. Phys. B 15, 2139 (1982).
9. D. Jürgens and V. Helbig, unpublished.
10. S.R. Goode and J.P. Deavor, Spectrochimica Acta 39B, 813 (1984).
11. E.E. Salpeter, Phys. Rev. 120, 1528 (1960).
12. T. Brandt, Thesis, Kiel (1983).